Effects of surface micro-structuring on the nucleation mechanisms

E. Teodori[1], A. S. Moita[1] e A. L. N. Moreira[1]

[1]IN+ - Departamento de Engenharia Mecânica, Instituto Superior Técnico, Universidade Técnica de Lisboa, Av. Rovisco Pais, 1049-001 Lisboa, Portugal
email: anamoita@dem.ist.utl.pt

Abstract

The use of surfaces with modified topography is often proposed to enhance pool boiling heat transfer. Recent studies have shown that several interaction mechanisms among the artificially created nucleation sites can deeply alter bubble dynamics, deteriorating the heat transfer coefficient. In this context, the present work addresses an approach of using regular micro-patterns to control such phenomena. Silicon surfaces are structured with arrays of square cavities, in which the distance among them is varied. High speed visualization is used to describe the boiling morphology and bubble dynamics. The enhancement of the heat transfer performance, obtained with the structured surfaces is evaluated based on the measured boiling curves and on the heat transfer coefficients. The results confirm a significant role of the interaction mechanisms and particularly of horizontal coalescence in the phenomenon of heat transfer coefficient deterioration. Two new parameters are suggested to relate the bubble dynamics (and consequently the surface topography) with the heat transfer coefficients: the modified dimensionless cavity spacing $(S.N_{cav} / N_{sites}) / \overline{D}_b$, which takes into account how the distance among nucleation sites changes with the heat flux and the coalescence factor $D^* = D_b/D_{nc}$ which provides a quantitative evaluation of the occurrence of horizontal coalescence. Deepening this analysis is expected to provide precise relations which allow a systematic optimization of the surface pattern leading to an effective heat transfer enhancement, for situations involving high heat fluxes.

Keywords: *Pool boiling; Square cavities; Bubble dynamics; Nucleation sites interaction; Immersion cooling and Modified dimensionless cavity spacing.*

1. INTRODUCTION

Nucleate pool boiling is a very effective form of heat transfer that has been widely used for cooling applications, particularly in high energy density systems, such as nuclear reactor power plants and electronic devices. Its effectiveness is due to the particular mechanism of heat transfer which involves three parcels, namely the natural convection from the heating surface to the fluid, the bulk convection induced by bubble growing and detachment and the vapour convection directly transferred into the bubble from the surface [1]. These parcels are influenced by several variables such as the bubble size, the departure frequency, the nucleation sites density, the thermo physical properties of the fluids and the surface topography, among others. So, one may stand that the heat transfer coefficient is a complex function of all of these variables. The complexity arises from the interdependency between the diverse variables. One of the variables which is easier to alter in a controllable way is the surface topography. This has been argued from many years as a strategy to improve the heat transfer coefficient in pool boiling. Altering surface topography has potentially two favourable effects: *i)* increase the liquid solid contact area and *ii)* increase the number of active nucleation sites, as the cavities in the surface act as preferential nuclei, promoting the appearance of active nucleation sites within the heterogeneous nucleation process [2]. While the first is an obvious benefit, the latter is not so straightforward, since a larger number of active nucleation sites should promote the bulk convection induced by bubble growing and detachment and the vapour convection. However, it also promotes several interaction mechanisms between nucleation sites, which may enhance the activity of the nucleation sites or actually inhibit it, so that the negative effects of such interaction can overcome the potential advantages. These interactions are particularly intense at high heat fluxes, which are the main target in the cooling of high energy density systems, so they must be well understood and controlled. The interaction phenomena caught the attention of pioneering researchers, such as Chekanov [3], Sultan and Judd [4] and more recently Zhang and Shoji [5]. The relation between the dimensionless cavity spacing $S/\overline{D_b}$ - i.e. the ratio of the cavity spacing to the average bubble departure diameter, and the average bubble departure frequency $\bar{f}_b$, were the parameters used to identify the different interaction regions. In the abovementioned studies, the authors tried to define interaction regions, as a function of the dimensionless cavity spacing$S/\overline{D_b}$, However, each author established different regions. The most unifying theory was proposed by Zhang and Shoji [5], who associated the interaction regions, also as a function of $S/\overline{D_b}$, with the relative

importance of three competitive effects, namely the hydrodynamic interaction between bubbles, the thermal interaction between nucleation sites and the horizontal and declining bubble coalescence. The main limitation of this study is the very limited number of cavities which turns difficult any extrapolation to the rough surfaces used in practical applications, which have numerous cavities. In this context, many subsequent works repeatedly used modified surfaces with a stochastic roughness (*e.g.* [6]). However, such surfaces can only be characterized with averaged roughness amplitude parameters, (such as the mean roughness R_a), which cannot be used to accurately describe the surface topography, as recently shown by Kotthof and Gorenflo [7] and Moita and Moreira [8]. As a result, many of these studies present contradictory results, based on trial-and-error approaches. Therefore, the present work stands for the use of micro-structures, such as microstuds (*e.g.* Mudawar and Anderson [9]), micro fins (*e.g* Honda *et al.*, [10]) and micro-cavities. These regular patterns are also very effective in enhancing boiling heat transfer and allow better understanding and control of the interaction mechanisms, since the surface topography is characterized by well defined quantities. In fact, very recent studies, based on a limited number of micro-cavities (*e.g.* [11,12]) allowed to relate the decline of the heat transfer coefficient observed at high heat fluxes (but still away from the Critical Heat Flux conditions) with the formation of large vapour bubbles, induced by the occurrence of horizontal coalescence among nucleation sites, which cover the heating surface. These vapour films decline the heat transfer, due to the low thermal conductivity of vapour and to the fact that they reduce the induced liquid motion. This suggests that especially for higher heat fluxes, an optimal pattern of the structural elements can be obtained, which besides augmenting the liquid/solid contact area, controls the inhibitive interaction among nucleation sites thus leading to an overall improved cooling performance. This may be so, since in recent work, Yu *et al.* 13] and of Nitesh *et a.l* [14] also suggest the establishment of an optimum inter-cavity spacing, for which most of the surface remains active for a wide range of heat fluxes, although they are not very clear on the arguments sustaining this optimum spacing.

In this context, the present work addresses a detailed study on the pool boiling processes on surfaces with a known and well defined number of artificially created cavities, to quantify the effect of the surface topography, on the interaction mechanisms, and particularly on the horizontal coalescence. At this stage of the research, all the parameters of the micro-pattern are fixed (size, shape and depth of the cavities) and only the spacing between cavities is varied, to allow a systematic approach. Two fluids are used (water and ethanol) in order to take into account also the effect of the liquids properties. Bubble dynamics is investigated as a function of the distance among cavities and is then correlated to the heat transfer coefficients. Two new parameters are suggested to establish this relation, namely the modified dimensionless cavity spacing $(S.N_{cav} / N_{sites}) / \overline{D}_b$ that takes into account how actually the distance among nucleation sites changes with the heat flux, and a coalescence factor $D^* = D_b/D_{nc,}$ which provides a quantitative evaluation of the occurrence of horizontal coalescence.

2. EXPERIMENTAL METHOD

2.1 Experimental arrangement

The experimental arrangement, which is schematically represented in Figure 1, mainly consists on a power supply, a heating block, a pool boiling test section, a high-speed camera (Phantom v4.2 from Vision Research Inc., with 512x512pixels@2100fps and a maximum frame rate of 90kfps) and a temperature acquisition system. Backlight illumination is provided by a 450W LED spotlight, passing through a diffusing glass to homogenize the background light.

Type-K thermocouples are used to monitor and acquire the temperature and evaluate the heat flux. The signals of the thermocouples are sampled with a National Instruments DAQ board plus a BNC2120 and amplified with a gain of 300 before processing. The acquisition frequency is 100Hz and the temperature is monitored for 20 seconds after reaching a stable condition of the system that in this case has been represented by a constant temperature variation of +-0.5°C. The heating module consists on a copper support, insulated by fibreglass and heated by two electric cartridge heaters. Different holes were drilled on the support in order to place the thermocouple at different known distance, and below the surface. The temperature distribution of the copper support has been evaluated by mean of temperature measurements with a range of imposed heat flux. The heat losses evaluated for this configuration are 37% in the worst case.

The micro-textured surfaces are placed on the top of the copper support. These surfaces, which have an area of $1cm^2$, are made from silicon wafers with a thickness of 0.380 μm.

The boiling section is directly built over the copper support. It has an area of 7.05cm^2 and a height of 15mm. The amount of liquid is 7ml.

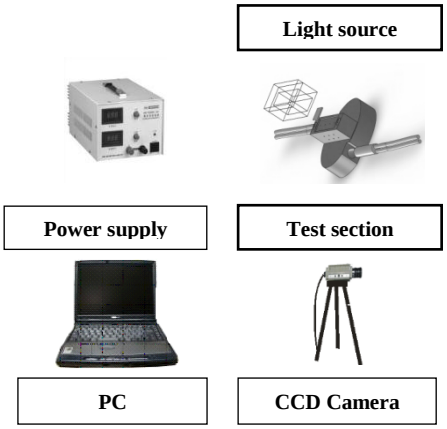

Fig. 1. Schematic layout of the experimental arrangement

2.2 Characterization of the micro-textured surfaces

From the numerous patterns which were custom made to determine the effect of the surface topography in the boiling mechanisms, the surfaces used in this study were micro-textured with square cavities. The patterns are custom made, combining wet etching with plasma etching. The size and depth of the cavities was fixed for this part of the study. So, the length of the squares is 20μm and the depth of the cavities is 30μm. The distance between the centres of the cavities *S*, is the variable and ranges between 200μm<*S*<2000μm. These quantities, which are defined in Figure 2, are measured directly from the roughness profiles, obtained using a mechanical profile meter, with a measurement precision of ±100Angstroms. The main topographical characteristics of the surfaces used here are summarized in Table 1.

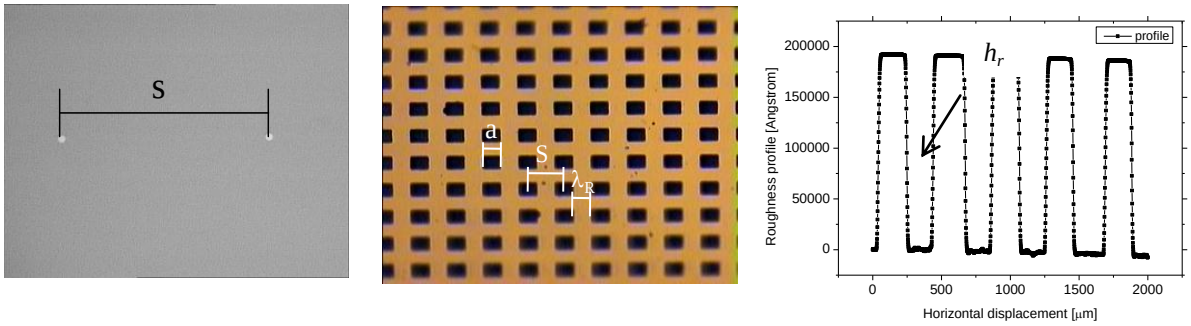

Fig. 2. Detail of a micro-textured surface showing the definition of the dimensions a, h_r, λ_R and S characterizing its topography.

Table 1. Summary of the main range of the topographical characteristics used in the customized micro-textured surfaces. Nc_{av} is the number of cavities in the entire surface.

Material	Reference	a [μm]	h_r [μm]	S [mm]	λ_R [μm]	N_{cav}
Silicon wafer	Smooth surface	≈ 0	≈ 0	≈ 0	≈ 0	≈ 0
	C3	127	30	304	177	1089
	C2	286	30	626	340	256
	C1	204	30	464	260	441

2.3 Methodology

The pool boiling is investigated for different liquids, namely ethanol and water, to account for the liquid properties as well as to infer on the additional effects of wettability in the observed phenomena. Qualitative and quantitative characterization of the various pool boiling regimes is achieved by combining high-speed visualization with temperature measurements and heat transfer calculations. Heat flux and heat transfer coefficients are determined for the various liquid/surface pairs. Afterwards, they are related to the bubble dynamics, which is quantified by the bubble departure diameter and frequency and active nucleation sites density. Table 2 depicts the thermo-physical properties of the liquids used in the present study.

Table 2. Thermo-physical properties of the liquids used in the present study, taken at saturation, at $1.013.10^5$Pa.

Property	Ethanol	Water
T_{sat} [°C]	78.4	100
ρ_l [kg/m^3]	736.4	957.8
ρ_v [kg/m^3]	1.647	0.5956
μ_l [mN m/s^2]	0.448	0.279
C_{pl} [J/kgK]	3185	4217
k_l [W/mK]	0.165	0.68
h_{lg} [kJ/kg]	849.9	2257
σ_l [N/m]	0.017	0.058

2.3.1 Pool boiling curves

Each boiling curve presented for every pair liquid-surface used here is averaged from seven experimental curves. The curves are obtained by varying the imposed heat flux in steps of 15W/cm^2. The temperature measurements are taken for each heat flux step when the system is considered to attain equilibrium, i.e. when the temperature oscillation is ±0.5 °C. Before each experiment the fluid is degassed by maintaining it in the pool at a temperature 20°C above the saturation temperature.

Experiments were conducted to obtain average boiling curves by both increasing and decreasing the heat flux, to infer on hysteresis effects, as pointed for instance by Mohamed and Bostanci (2002). The temperature measures have an uncertainty of ±1°C. The relative error associated with the determination of the heat transfer is 5%.

2.3.2 Bubble nucleation parameters

Following the approach presented in the most of the works reported in the literature the bubble nucleation parameters selected in the present study are the bubble departure diameter, the bubble departure frequency and the active nucleation sites density. This characterization is based on high-speed visualization and image post-processing. The images are recorded with a frame rate of 2200fps. For the optical configuration used here, the spatial resolution is 9.346μm/pixel.

The bubble departure diameter is measured for each test condition from 300 to 1060 frames, which were recorded at 2200 fps. For each image a mean value is averaged from 5-16 measurements for every nucleation site that is identified in the frame.

At higher heat fluxes, the various interaction mechanisms, which will be discussed in the following section may alter significantly the value of the departure diameter, especially when horizontal coalescence occurs.. Therefore, in those cases, the measured diameters are a mean value taken from the averaged diameters, which are evaluated after the occurrence of such events and the one evaluated without taking into account such events.

The error associated to the measurements of the bubble departure diameter is of ±1 pixel, corresponding to ±9.346 μm.

The bubble departure frequency is estimated by determining the time elapsed between apparent departure events, which are counted for a defined interval of time. The departure frequency is assessed, for each test condition, for at least five nucleation sites, which are evaluated based on extensive image post-processing of 300 to 1060 frames, which were recorded with a frame rate of 2200fps. The final value of the bubble departure

frequency is the average between the frequencies of each nucleation site. The uncertainty associated to these measurements is ±1 fps.

Finally, the evaluation of the active nucleation sites density must be done by visual inspection of the frames, which introduces an uncertainty associated to the subjective criterion of the observer. To lessen this uncertainty, at least ten frames are chosen, at different times during the single experiment. The final values of the active nucleation site density are an average of the ten evaluated values. The uncertainty introduced in the visual identification of the nucleation sites by the chaotic behaviour of the boiling phenomenon was assessed in the "worst scenario" to be ±18%.

3. RESULTS

3.1 Boiling morphology

As argued in the introduction, the interaction among nucleation sites and particularly the horizontal coalescence can alter significantly the heat transfer process and consequently the heat transfer coefficients in the pool boiling. Therefore, one must analyse the boiling morphology and how it is affected by the surface topography, combined with the liquid properties. The region of interest lays in the working conditions for which the imposed flux is close to the critical heat flux of the pool. This is obvious, since in most cooling applications (for instance of electronic components) the system to cool can be damaged if the imposed heat flux overcomes the critical one. Thus, in this range a very precise control of the heat transfer must be achieved, for which the surface topography plays a vital role. Such role is illustrated in Figures 3 and 4 which depict the boiling morphology of water and ethanol, respectively, at high heat fluxes, for different surfaces in which the cavities are spaced at various *S*. Water and ethanol are chosen due to the significant differences in the surface tension of the liquids (see Table 2), which is associated to different boiling morphologies, as previously discussed in [12].

A close inspection of Fig. 3 highlights that for water pool boiling, very large and deformed bubbles depart from the surface. These large bubbles are a consequence of horizontal coalescence, as explained also in [12]. This strong coalescence is attributed to the liquid properties and most especially to the large surface tension of water, which leads to a more violent and chaotic boiling behaviour, with average larger departure diameters. Also, the surface tension keeps the formed bubbles attached to the surface for longer, further promoting horizontal coalescence. Obviously, horizontally coalesced bubbles result in larger flow resistance, precluding the rewetting of the liquid into the cavities and delays even more bubbles departure. So, playing with the distance between the cavities, *S* weighted by the average departure diameter, $S/\overline{D_b}$ as suggested by [5] can be an effective way to control the unwanted overstated horizontal coalescence. However, while [5], restricted their study to two cavities, in this case, similarly to what will occur in a practical application, the structured area is larger, so one must also take into account the number of cavities.

Concerning the pool boiling of ethanol, as shown in Fig. 4., given the much smaller surface tension of this liquid, the bubbles departing from the surface are quite small, when compared to those of water and the bubbles population is homogeneously distributed all over the surface. The horizontal coalescence is therefore less evident, so that only very mild differences can be observed when comparing the boiling over different surfaces.

(a) **(b)** **(c)**

Fig. 3. Water boiling morphology on structured surfaces: (a) Surface C1 Heat flux 38.15 W/cm^2 ΔT=19.75.(b) Surface C2 Heat flux 47.789 W/cm^2 ΔT=21.34 (c) Surface C3 Heat flux 36.05 W/cm^2 ΔT=16.02.

(a) **(b)** **(c)**

Fig. 4. Ethanol boiling morphology on structured surfaces: (a) Surface C1 Heat flux 22.88 W/cm^2 ΔT=21.64 (b) Surface C2 Heat flux 26.88 W/cm^2 ΔT=20.24 (c) Surface C3 Heat flux 32.13 W/cm^2 ΔT=23.44.

So, it is evident that the effect of the surface topography on the coalescence is easier to be observed on a liquid like water, with larger surface tension. However, the boiling mechanisms of the liquids with smaller surface tension are similar. Hence, independently of the fluid, the relevant quantities which can be correlated between the surface and the boiling mechanisms (focusing on horizontal coalescence occurring at high heat fluxes) are the same: $S/\overline{D_b}$ and number of active cavities.

3.2 Relation between bubble nucleation and the heat transfer coefficient

The morphological analysis briefly presented in the previous paragraphs suggests stronger coalescence effects occurring on the pool boiling of the liquid with larger surface tension. A strong coalescence effect will easily lead to the formation of large vapour bubbles, which result in the deterioration of the heat transfer coefficient. To quantify how strong is the horizontal coalescence among nucleation sites we propose to analyse the coalescence factor $D^*= D_b/D_{nc}$, defined by the ratio between the average bubble departure diameter (including coalescence) and the single diameter of the bubbles which exit the cavity with no coalescence. Obviously this factor increases with the heat flux as well as with the occurrence of horizontal coalescence, taking into account that a value equal to 1 means that there is no coalescence among nucleation sites. Fig. 5 (a) reports the coalescence factor versus the heat flux for water. D^* is always larger than 1, clearly indicating a strong coalescence effect. Furthermore the Figure shows that the surface C3, with the denser cavities is the one that presents the highest values of D^* meaning that the topography of this surface is promoting the coalescence. The other two surfaces instead present almost the same values of D^*, as the distance between the cavities is similar.

On the other hand the effect of coalescence is much less evident with the ethanol, the liquid with the smallest surface tension, as the D^* is almost always equal to 1 and only a slight increase can be seen for higher values of heat fluxes (Fig. 5b). The effect of the surface topography here is also not significant so, if the coalescence effect is indeed important to deteriorate the heat transfer coefficient, one may argue that the distance between cavities can be further reduced in order to increase the number of nucleation sites.

In order to quantify the effect of coalescence in the heat transfer coefficient, one must start by understanding its influence on the bubble dynamics. So, quantitative description of the bubble dynamics is reported in Fig. 6, which depicts the bubble departure diameter, the nucleation sites density and the bubble departure frequency, for the pool boiling of water over different patterns (different distance *S* between the cavities's centers). The measured bubble departure diameters increase with the heat flux, as expected. Comparing the different surfaces, the departure diameter is smaller as one decrease the distance between the cavities, because, particularly for high heat fluxes, which are the focus of interest in this paper, the size of the formed bubbles easily reaches values for which close distance between the cavities will promote the horizontal coalescence.

The nucleation sites density also increases with the imposed heat flux, as it is easier to activate the artificial cavities. Since one of the major advantages of creating surface roughness is to create more nucleation sites to improve the convective heat transfer due to the convection induced by bubble motion e.g.[1] one may argue that the surface with smaller *S* should perform better. However, Fig. 5 shows that the surface with smaller *S* is also promoting a very strong horizontal coalescence, so one must weight both effects.

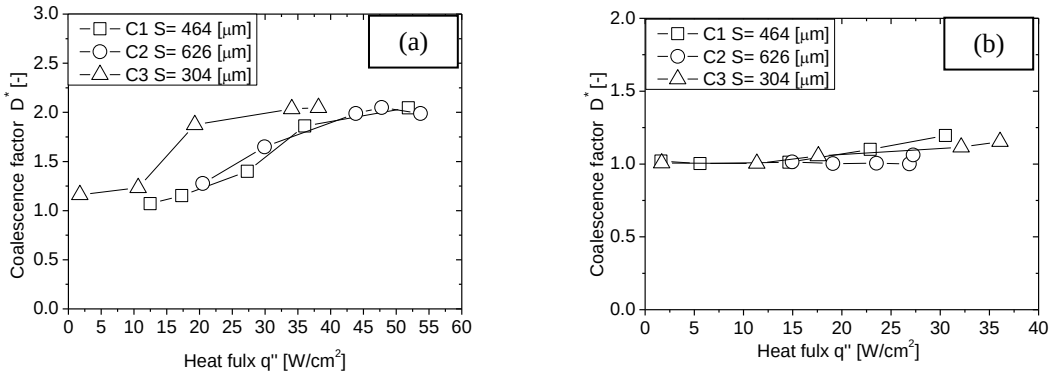

Fig. 5. Coalescence factor versus heat flux for: (a) water (b) ethanol.

This may be easier to understand looking at the departure frequency. At lower imposed heat fluxes, an increase of the heat flux will activate the nucleation sites favouring bubble departure (and indirectly the heat transfer due to the motion of the bubbles). Such trend will proceed until a maximum value, after which the frequency decreases. This maximum sets the condition after which the effect of the horizontal coalescence becomes dominant and the frequency rapidly decreases, as one tries to further increase the imposed heat flux. Since the frequency is related to the velocity of the departure bubbles, higher frequency will promote convection. This is expected, as the heat transfer coefficient h is quite affected by the induced bubble motion so that it is a function of the Reynolds number. Looking at the plots in Fig. 6 one observe that the surface allowing to reach higher maximum of the frequency departure is not either the one with highest distance *S*, (C2) which would preclude for sure the horizontal coalescence, neither that with the densest nucleation sites (C3). So, there is definitely a competition between these effects which must be weighted. For that propose, we suggest here a new dimensionless cavity spacing $(S.N_{cav} / N_{sites}) / \overline{D}_b$ where S is the distance between cavities' centres, N_{CAV} is the cavities density on the surface, N_{ACT} active nucleation sites density and D_b is bubble departure diameter. The distance among nucleation sites is actually the distance among cavities only when 100% of them are active. Otherwise a homogeneous distribution of the active nucleation sites is assumed. This assumption is valid for high heat fluxes, which are the main focus of the present paper. Further research is now required to adequate this parameter with a modified distribution of N_{CAV}/N_{ACT}, for lower imposed heat fluxes, which is out of the scope of this paper. The probabilistic distribution of the active nucleation sites for a variable range of low heat fluxes is quite complex and only recently a few studies started to focus on this topic *e.g.* [15].

The bubble departure frequency and the heat transfer coefficient are plotted versus the modified dimensionless cavity spacing in Figs. 7 (a) and (b), respectively.

From these Figures it can be observed that the bubble departure frequency and the heat transfer coefficient present almost the same trend with the modified dimensionless cavity spacing. This is due to the aforementioned relation between the heat transfer coefficient and the Reynolds number. Decreasing $(S.N_{cav} / N_{sites}) / \overline{D}_b$, by augmenting the imposed heat transfer will favour the convection due to a higher departure frequency. For the range of surfaces studied here, a maximum occurs in all of them for $0.56<(S.N_{cav} / N_{sites}) / \overline{D}_b<0.78$. Afterwards, the steep descent of both bubble frequency and h is related to the horizontal coalescence leading to the formation of a vapour blanket which insulates the surface and precludes the fluid circulation. Following this argument, the surface endorsing the highest frequency maximum is also promoting the highest heat transfer coefficient for a given (high) imposed heat flux (in this case, surface C1). The representation based on the dimensionless cavity spacing clearly highlights the strong influence of the coalescence effect endorsed by surface C3 in the deterioration of the heat transfer coefficient.

This study is yet preliminary, so that a wider range if the modified dimensionless cavity spacing for fixed values of the heat transfer must be investigated. However, it seems that this parameter can lead to find an optimal surface topography (according to the liquid studied), to control the horizontal coalescence. Indeed looking at the boiling curves and correspondent heat transfer coefficients, as depicted in Fig. 8, for the range of patterns studied here, the pattern C1 is the one leading to the highest heat transfer coefficients. It is also the pattern for which the

decay of the heat transfer coefficient, which is associated to the formation of the vapour blanket [12] occurs later i.e., at higher heat fluxes.

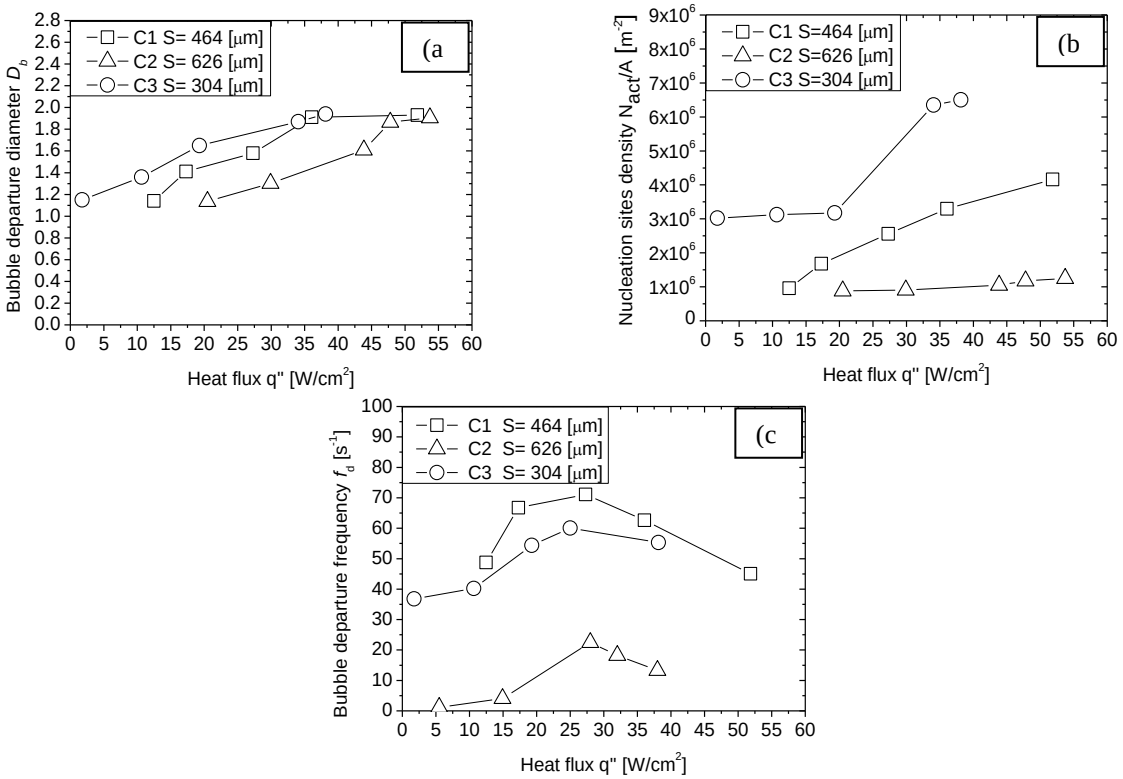

Fig. 6. Water bubble dynamic on structured surfaces: (a) Bubble departure diameter versus heat flux (b) Nucleation sites density versus heat flux (c) Bubble departure frequency versus heat flux.

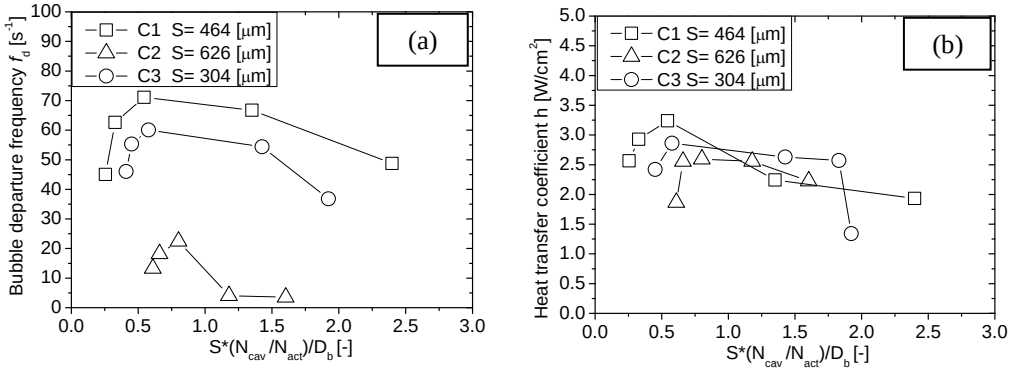

Fig. 7. Evaluation of the interaction among nucleation sites for water: (a) Bubble departure frequency versus the modified dimensionless cavity spacing; (b) Heat transfer coefficient versus modified dimensionless cavity spacing.

The discussion presented up to now addresses only the liquid with the highest surface tension, for which the effect of the horizontal coalescence is more evident. A similar analysis is now required to the pool boiling of the liquid with the smaller surface tension. Fig. 9 shows the measured bubble departure diameters, active nucleation sites density and bubble departure frequency, as a function of the heat flux, for the pool boiling of ethanol.

Also for this liquid, the bubble departure diameters increase with the heat flux (Fig. 9a).However, it is clear that the characteristic size of the bubbles is much smaller when compared to that of the water, as reported in Fig.

5(a). Since for comparison purposes the same patterns are used with both liquids, the effect of the pattern is now less evident because the distance *S* is still quite large, so that a strong horizontal coalescence does not occur. Similarly to what was discussed for the water, the number of active nucleation sites, represented in Fig. 9 (b) is the highest for the pattern with smallest *S*, which has more cavities. The boiling of ethanol is much more homogeneous, which associated to a lower effect of horizontal coalescence leads to a slightly different behaviour of the bubble departure frequency, shown in Fig. 9 (c). So, the influence of altering the parameter *S*, for the ranges used in this study, is not significant, simply because it is not yet within a range for which the horizontal coalescence is relevant.

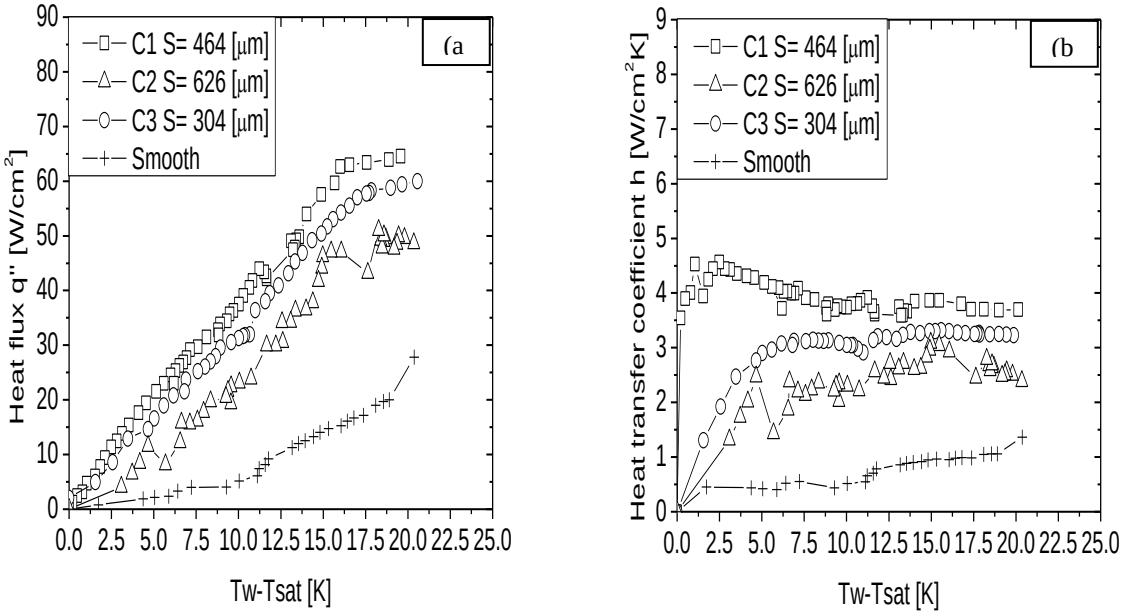

Fig. 8. Water boiling curves on structured surfaces: (a) heat flux versus wall superheat (b) heat transfer coefficient versus wall superheat.

The mild slowing down of the bubble departure frequency is basically due to the fact that it is gradually more difficult for the liquid to rewet the surface for higher heat fluxes. At the limit the high frequency will itself preclude the rewetting.

Performing now the analysis which relates the heat transfer coefficient with the departure frequency and with the modified dimensionless cavity spacing $(S.N_{cav} / N_{sites}) / \overline{D}_b$, as reported in Figs. 10 (a) and (b), the effect of the pattern is again easier to understand.

The Figures show an over positioning of all the curves, as the effect of the distance *S* is not significant. The trend of the modified dimensionless cavity spacing however suggests that the maximum value (which was detected for the water) has not been yet achieved. So, the curve for the surface with the largest S is almost constant, as this is closest to a smooth surface, so that a maximum value is not perceptible. Instead the frequency keeps increasing for rising values of the heat flux (in the direction of smaller values of the modified dimensionless cavity spacing), because the distance between the cavities is not yet small enough to be compared to the size of the bubbles. This is particularly evident for the pattern with the smallest *S*, (surface C3) which leads to a significant boost of the frequency (and consequently of the heat transfer coefficient) for quite small values of the modified dimensionless cavity spacing, which are associated to higher heat fluxes. In agreement to this, the boiling curves and heat transfer coefficients obtained for the various surfaces, are quite close to each other. The curve obtained with for the micro-pattern with the largest *S* is almost coincident with that measured for the smooth surface, which is consistent to the "smoothing" behaviour generated by this surface, as discussed in the previous paragraph. Also, consistently from the analysis based on the modified dimensionless cavity spacing, the surface C3 is providing the best performance, as shown in Figure 11.

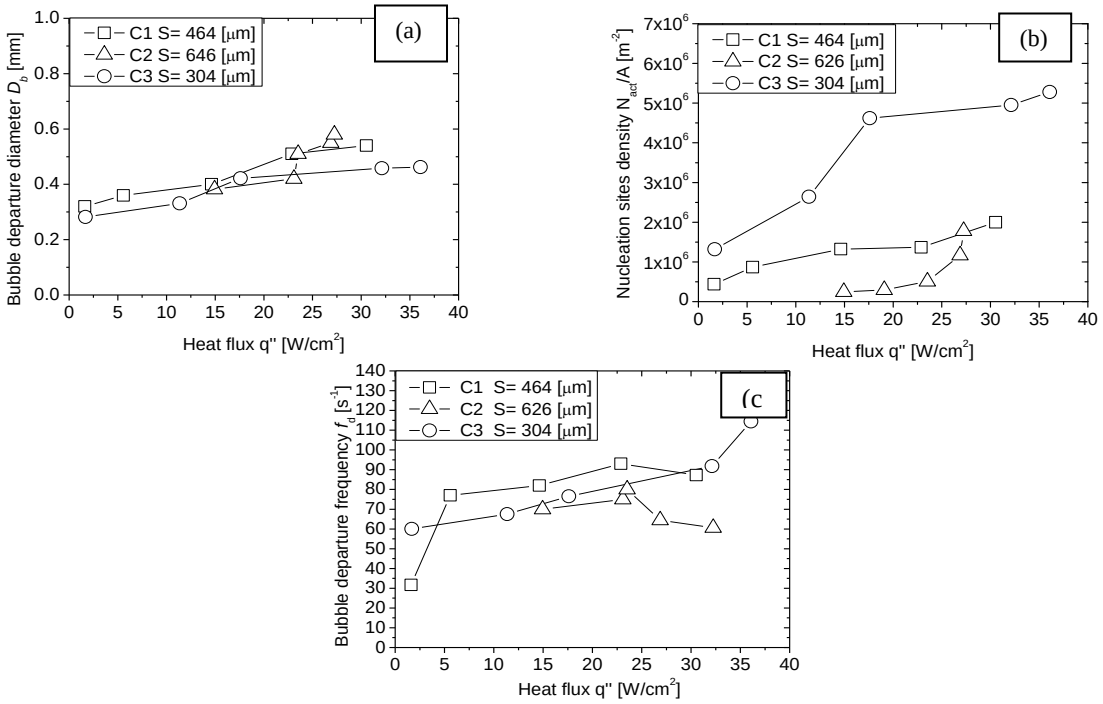

Fig.9. Ethanol bubble dynamic on structured surfaces: (a) Bubble departure diameter versus heat flux (b) Nucleation sites density versus heat flux (c) Bubble departure frequency versus heat flux.

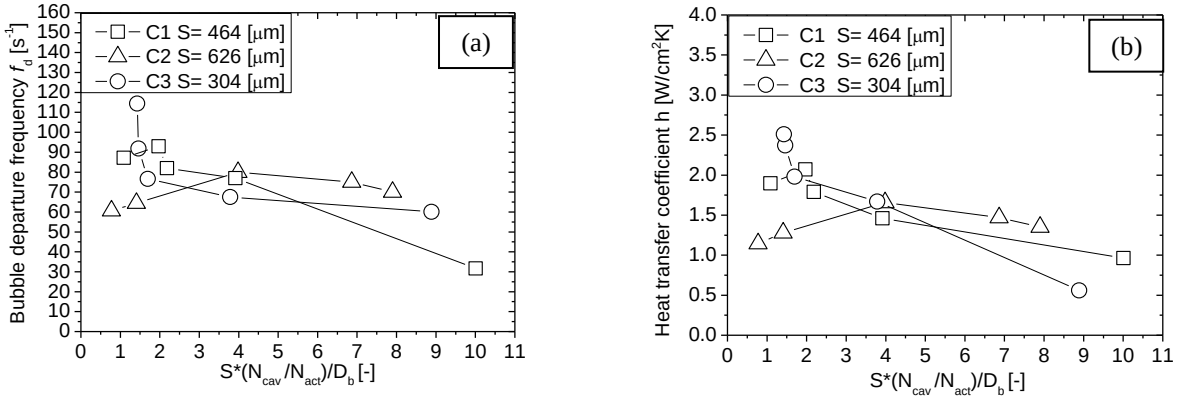

Fig. 10. Evaluation of the interaction among nucleation sites for water: (a) Bubble departure frequency versus modified dimensionless cavity spacing (b) Heat transfer coefficient versus modified dimensionless cavity spacing.

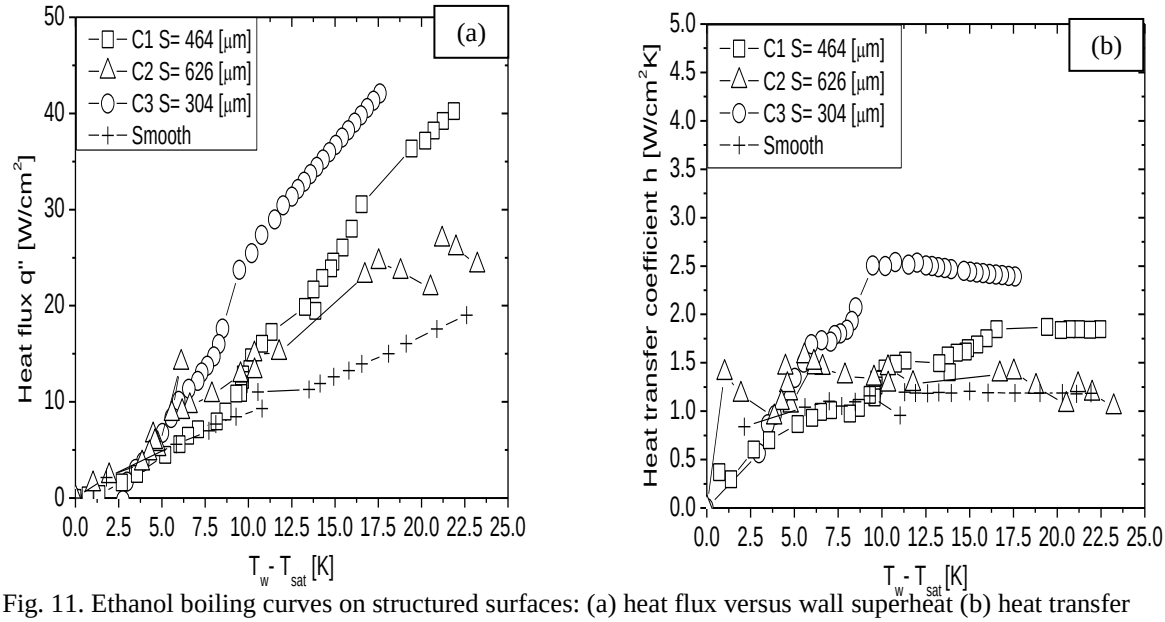

Fig. 11. Ethanol boiling curves on structured surfaces: (a) heat flux versus wall superheat (b) heat transfer coefficient versus wall superheat.

4. FINAL REMARKS

The present paper focus on the relation between the bubble dynamics and the heat transfer coefficients, for liquid pool boiling over micro-textured surfaces. The micro-textures are composed by arrays of a well defined number of square micro-cavities. For this stage of the research, all the parameters of the micro-pattern are fixed (size, shape and depth of the cavities) and only the spacing between cavities is varied, to allow a systematic approach. Bubble dynamics is investigated as a function of the distance among cavities and is then correlated to the boiling curves and to the heat transfer coefficients. Interaction among nucleation sites is quantitatively described using a new parameter, the coalescence factor $D^* = D_b/D_{nc}$, defined by the ratio between the average bubble departure diameter (including coalescence) and the single diameter of the bubbles which exit the cavity with no coalescence. The results indicate that, for high heat fluxes, achieving high heat transfer coefficients is a compromise between increasing the density of active nucleation sites, (thus promoting the induced convection) and controlling the interaction mechanisms, namely the horizontal coalescence, which may lead to the formation of large vapor bubbles, which deteriorate the heat transfer coefficient. The role of the horizontal coalescence is particularly relevant in the pool boiling of liquids with large surface tension, such as water. Under these conditions, the modified dimensionless cavity spacing $(S.N_{cav} / N_{sites}) / \overline{D}_b$ is suggested to be useful to relate the coalescence effects with the heat transfer coefficients, as a function of the spacing between the cavities and the density of active nucleation sites. Based on these two new quantities, the results show that for the water the patterns used so far are already within a range for which the optimization of the distance between cavities must account for the effect of horizontal coalescence, so there is a minimum cavity spacing leading to a maximum of the heat transfer coefficient. Afterwards, the formation of coalesced large bubbles becomes dominant in causing the deterioration of the heat transfer coefficient. Instead, for ethanol the analysis based on these two parameters indicates that the maximum value detected for the experiments with the water was not achieved yet, the suggesting that one may still decrease the spacing between cavities and therefore increase the density of active nucleation sites.

5. ACKNOWLEDGMENTS

The authors acknowledge the contribution of Fundação para a Ciência e a Tecnologia (FCT) by supporting A. S. Moita with a Fellowship (Ref.:SFRH/BPD/63788/2009).

The authors are also grateful to FCT for partially financing the research under the framework of project PTDC/EME-MFE/109933/2009 and for supporting E. Teodori with a research grant.

REFERENCES

1. Chi-Yeh Han, Peter Griffith, The mechanism of heat transfer in nucleate boiling, *Techincal Report No 7673-19*, Departement of Mechanical Engineering, Massachusets Institute of Technology, 1962.
2. C. Corty, A.S. Foust, Surface variables inn nucleate boiling, *Chem.Eng.Progress.Symo Ser*. 51(17)1-12,1955.
3. V.Chekanov, Interaction of centers during nucleate boiling, *Teplofizika Vysokikh Temperature* 15,121-128,1977.
4. A.Calka and R.L Judd, Some aspects of interaction among nucleation sites, *Journal of Heat Transfer – Transection of the ASME*, 102(3) 461-464,1985.
5. L.Zhang, M. Shoji, Nucleation sites interaction in pool boiling on the artificial surface, *International Journal of Heat and Mass Transfer*, 46(3)513-522, 2003.
6. B.J.Jones, J.P. McHale, S.V.Garimella, The influence of surfaace roughess on nucleate boiling heat transfer, *Journal of Heat Trasnfer*, 131/121009-1-14,2009
7. S.Kotthoff, D.Gorenflo, Heat transfer and bubble formation on horizontal copper tubes with different diameters and roughness structures, *Heat and Mass Transfer*, 45 893-908, 2009
8. A.S. Moita, A.L.N. Moreira, Scaling the effects of surface topography in the secondary atomization resulting from droplet/wall interactions, *Journal of Experiments in Fluids* 1-17, 2011
9. T.M. Anderson, I.Mudawar, Microelectronic cooling by enhanced pool boilling of a dielectric fluorocarbon liquid, *ASME Journal of Heat Transfer* 111 752-759, 1989
10. H. Honda, H. Takamastu, J. J. Wei, Enhanced boiling of FC-72 on silicon chips with micro-pin-fins and submicroscale roughness, *ASMe Jounarl of Heat Transfer* 124 383-390, 2002
11. J.P. McHale, S.V. Garimella, Bubble nucleation characteristics in pool boiling of wetting liquid on smooth and rough surfaces, *International Journal of Multiphase Flow*, 36 249-260, 2010
12. A.S. Moita, E.Teodori, A.L.N. Moreira, Influence of surface topography and wettabiblity in the boiling mechanisms, *ILASS 24th Annual Conference on Liquid Atomization ans Spray Systems*, Estoril, Portugal. 2011.
13. C.K. Yu, D.C. Lu, T.C.Cheng, Pool boiling heat transfer on artificial micro-cavity surfaces in dielectric fluid FC-72, *Journal of Micromechanics and Microenginnering* 16 2092-2099, 2006
14. D. N. Nimkar, S.H. Bhavnani, R.C. Jaeger, Effect of nucleation sites spacing on the pool boiling characteristics of a structured surface, *International Journal of Heat and Mass Transfer* 49 2829-2839, 2006
15. T.G. Karayiannis *et al*, Steps towards the development of an experimentally verified simulation of pool nucleate boiling on a silicon wafer with artificial sites, *Applied Thermal Engineerig*, 29 1327-1337, 2009.